Journal of Alloys and Compounds 495 (2010) 265–267

Contents lists available at ScienceDirect

Journal of Alloys and Compounds

journal homepage: www.elsevier.com/locate/jallcom

Effect of Ni concentration on the structure and magnetic properties for nanocrystalline Fe–Ni–N thin films

L.L. Wang[a,b], W.T. Zheng[b,*], T. An[a], N. Ma[b], J. Gong[a]

[a] College of Science, Changchun University, Changchun 130022, China
[b] Department of Materials Science and Key Laboratory of Automobile Materials of MOE, State Key Laboratory of Superhard Materials, Jilin University, Qianjin Street 2699, Changchun 130012, Jilin, China

ARTICLE INFO

Article history:
Received 24 November 2009
Received in revised form 26 January 2010
Accepted 29 January 2010
Available online 6 February 2010

Keywords:
Nanocrystalline γ′-$(Fe_{1-x}Ni_x)_4N$
Structure
Magnetic properties

ABSTRACT

Nanocrystalline γ′-$(Fe_{1-x}Ni_x)_4N$ (x = 0.05–0.50) thin films were synthesized on single crystal Si(1 0 0) substrates by facing target (Fe and Ni) magnetron sputtering at a mixture of Ar/N_2 gas discharge, and their Fe/Ni atomic ratio, structure, morphology, and magnetic properties at room temperature were characterized using X-ray diffraction (XRD), scanning electron microscopy (SEM), and vibrating sample magnetometer (VSM). The sputtering current for Ni target was fixed at 0.02, 0.04, 0.06, 0.08, 0.10 and 0.15 A, respectively, upon keeping the sputtering power for Fe target constant at 36 W (I = 0.10 A, U = 360 V). Via optimizing Ni concentration through varying sputtering current for Ni target, the structural stability and the soft magnetic properties for the films were improved effectively. As the Ni concentration for the films increased, their lattice parameters and saturation magnetization M_s decreased, while grain sizes increased. The coercive force H_c for the films decreased from 66 to 36 Oe as the Ni concentration increased from 0.05 to 0.36, but increased to 76 Oe with a further increase in Ni concentration up to 0.50.

1. Introduction

Iron nitride films have received much attention because of their excellent magnetic properties [1–8] and their ability to improve surface hardness and wear resistance [9] for application in magnetic devices. The γ′-Fe_4N phase has the face-centered cubic iron lattice with a nitrogen atom positioned at the body-center site, a better chemical stability which has been considered to be a potential candidate for a high-density recording material [10–12]. Up to now, how to obtain a single-phase γ′-Fe_4N has been concentrated on [13–15], including our previous work [16], in which the single-phase γ′-Fe_4N magnetic films have successfully been obtained by magnetron sputtering. However, Fe–N films show a high magnetostriction and poor thermal stability, and their good soft magnetic properties disappear with increasing annealing temperature owing to the grain growth of the refined iron. The addition of the third element into Fe–N to form ternary Fe–M–N films (M = Ta, Zr, Hf, Nb, etc.) [17–22] succeeds in solving the soft magnetic and thermal stability problems. Kopcewicz et al. [19] have studied the role of alloying elements such as Cr, Al, Ti and Mn, in the formation and stability of the nitride phases using conversion electron Mössbauer spectroscopy and found that the presence of alloying elements, especially Ti, significantly extends the range of the thermal stability of α″-martensite at low N doses and γ′-Fe_4N at high N doses toward higher temperatures. Panda and Gajbhiye [20] have synthesized nanocrystalline γ-Fe–Ni–N systems using the borohydride reduction route and the roles of interstitial nitrogen and fine particle size and surface effects have been studied with regard to the structure and magnetic properties. Some groups [23–28] have reported the dependence of the saturation magnetization, lattice parameter or coercive field on the Ni content for other nanocrystalline FeNiN compounds. However, a systematic study of the effect of introducing Ni element on the grain size, structure, and magnetic properties for γ′-Fe_4N phase need to be explored deeply. In this work, the Ni concentration dependent structural and magnetic properties for nanocrystalline γ′-$(Fe_{1-x}Ni_x)_4N$ films will be explored.

2. Experimental

Fe–Ni–N thin films were deposited on single crystal Si(1 0 0) substrates at 250 °C, discharging a mixed Ar/N_2, using facing target magnetron sputtering system (DPS-III), in which the base pressure was 9×10^{-5} Pa. Prior to deposition, the substrate was cleaned ultrasonically in acetone and alcohol consecutively. During deposition, the Fe target sputtering power was kept constant at 36 W (I = 0.1 A, U = 360 V), and the sputtering current for Ni target was fixed at 0.02, 0.04, 0.06, 0.08, 0.10 and 0.15 A, respectively. The pure argon (99.999) and nitrogen (99.999) gases were inlet into the chamber, controlled by two independent mass-flow controllers. The nitrogen fraction in whole gas flow rate was 7%, and the total pressure was fixed at 0.5 Pa. The sputtering time was controlled at 40 min, and the deposition rate is about 0.2 nm/s.

* Corresponding author. Tel.: +86 0431 85168246; fax: +86 0431 85168246.
E-mail address: WTZheng@jlu.edu.cn (W.T. Zheng).

0925-8388/$ – see front matter © 2010 Elsevier B.V. All rights reserved.
doi:10.1016/j.jallcom.2010.01.146

Table 1
Fe/Ni atom ratio, lattice parameter, H_c, M_s for γ′-$(Fe_{1-x}Ni_x)_4N$ thin films deposited using different sputtering currents for Ni target.

	Sample			
	(a)	(b)	(c)	(d)
Ni sputtering current (A)	0.02	0.04	0.06	0.10
Fe/Ni (atom ratio)	0.95:0.05	0.75:0.25	0.64:0.36	0.50:0.50
Lattice parameter (nm)	0.3782	0.3733	0.3722	0.3708
H_c (Oe)	66	45	36	76
M_s (emu/g)	166	153	156	144

The structure of the films was analyzed by X-ray diffraction (XRD) with Cu Kα radiation using a current of 200 mA and voltage of 40 kV (Rigaku, D/max-2500/PC). The morphology and composition of the films were characterized by scanning electron microscopy (SEM) (JEOL-6700F). Magnetic properties of the film were measured under the condition that the magnetic field was parallel to the film surface by vibrating sample magnetometer (VSM) (LakeShore 7407, USA), and the mass of the sample was obtained using electronic balance (AG249) for evaluating the saturation magnetization.

3. Results and discussion

3.1. Film composition

SEM energy spectroscopy is used to evaluate the composition for the Fe–Ni–N films deposited employing different sputtering currents (0.02, 0.04, 0.06, and 0.10 A, respectively) for Ni target, and the results are listed in Table 1, in which the Ni concentration (x-value) increases with increasing sputtering current for Ni target. The Ni concentration (x-value) for the film grown at the sputtering current for Ni target of 0.02, 0.04, 0.06, and 0.10 A is 0.05, 0.25, 0.36, and 0.50, respectively, and the Fe/Ni atomic ratio is close to 0.5:0.5 as the sputtering current for both Ni and Fe target is 0.1 A.

3.2. Film structure

Fig. 1 shows the XRD patterns for the Fe–Ni–N films deposited on single crystal Si(1 0 0) substrate at 250 °C with different sputtering currents for Ni target, where except the peaks at $2\theta = 33.05^\circ$ and $2\theta = 69.42^\circ$ which result from Si(2 0 0) and (4 0 0) substrate, the other two peaks at $2\theta = 41.32^\circ$ and 47.88° correspond to γ′-Fe_4N(1 1 1) and (2 0 0), respectively, which means that a single-phase γ′-Fe_4N crystal structure is obtained in the film. The peak position in Fig. 1 almost accords with that from the standard powder diffraction files (PDF) regardless of whether Ni element is introduced or not, indicating that the γ′-$(Fe_{1-x}Ni_x)_4N$ films are obtained. Fig. 1(a)–(d) exhibits that the diffraction peaks (1 1 1) and (2 0 0) for γ′-$(Fe_{1-x}Ni_x)_4N$ films move toward the large-angle side with increasing Ni concentration (x-value). For instance, in Fig. 1(d) ($x = 0.50$), the γ′(1 1 1) and (2 0 0) peaks for γ′-$(Fe_{1-x}Ni_x)_4N$ film at $2\theta = 42.24^\circ$, 49.20° move toward large-angle side by 0.92° and 1.32°, respectively, compared to those in Fig. 1(a) ($x = 0.05$). The decrease in the lattice parameter for γ′-$(Fe_{1-x}Ni_x)_4N$ films, upon introducing Ni, can be readily understood since the atomic radius of Ni ($r_{Ni} = 0.125$ nm) is slightly smaller than that of Fe ($r_{Fe} = 0.127$ nm). For the film with Ni concentration equal to or larger than 0.50 ($x \geq 0.5$), the new peak at $2\theta = 44.04^\circ$ from Fe(1 1 0) or Ni(1 1 1) appears in Fig. 1(d) and (e), which implies that a mixture of phases including both γ′-$(Fe_{1-x}Ni_x)_4N$ and Fe(1 1 0) or Ni(1 1 1) exists in the film as Ni concentration is too high. The calculated lattice parameters, using diffraction peaks (1 1 1) of γ′-$(Fe_{1-x}Ni_x)_4N$, are listed in Table 1, from which the lattice parameters for γ′-$(Fe_{1-x}Ni_x)_4N$ films decrease with increasing Ni concentration, and are smaller than the value $a = 0.3790$ nm for γ′-Fe_4N reported by Jacobs [15]. The lattice parameter values and the dependence on Ni content can also be found in FeNiN films reported by Diao et al. [25].

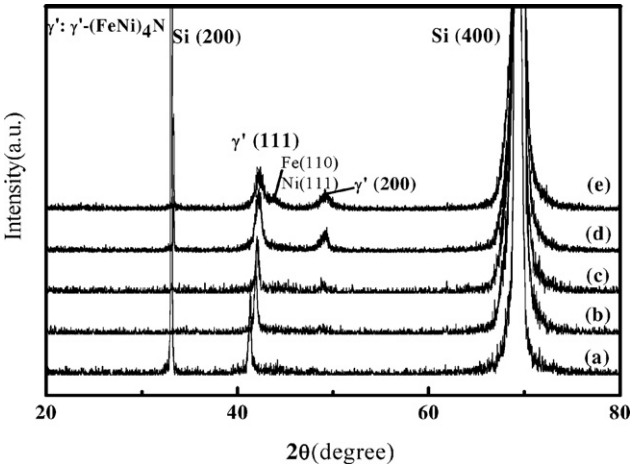

Fig. 1. XRD patterns for γ′-$(Fe_{1-x}Ni_x)_4N$ thin films deposited using sputtering current for Ni target of (a) 0.02, (b) 0.04, (c) 0.06, (d) 0.10 and (e) 0.15 A, respectively.

3.3. Film morphology

Fig. 2 displays the SEM image for the γ′-$(Fe_{1-x}Ni_x)_4N$ film deposited on single crystal Si(1 0 0) substrates at 250 °C with different Ni concentrations, where the triangle pyramid shape of γ′-$(Fe_{1-x}Ni_x)_4N$ grains can be clearly observed as Ni concentration is $x = 0.05$ in Fig. 2(a), and the average grain size is evaluated about 55 nm, which means that the obtained γ′-$(Fe_{1-x}Ni_x)_4N$ film is nanocrystalline. The grain sizes of the sample increase with increasing Ni concentration, which may be ascribed to that a high sputtering current for Ni target may favor the grain growth. Also, the grain shape has been changed from the triangle pyramid to rhombic with increasing Ni concentration, which can be due to the appearance of pure Fe or Ni phase in the film.

3.4. Film magnetic properties

Fig. 3 exhibits the magnetic hysteresis loops for the γ′-$(Fe_{1-x}Ni_x)_4N$ thin films with different Ni concentrations, and the values of saturation magnetization and coercivity are listed in Table 1, from which the γ′-$(Fe_{1-x}Ni_x)_4N$ film has a soft magnetic characteristic. From Fig. 3(a), for the film with $x = 0.05$, the saturation magnetization is about 166 emu/g and the coercivity

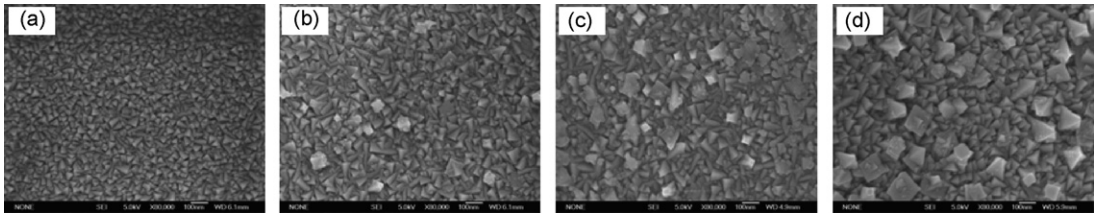

Fig. 2. SEM images for γ′-$(Fe_{1-x}Ni_x)_4N$ thin films with Ni concentration (x-value) of (a) 0.05, (b) 0.25, (c) 0.36, and (d) 0.50, respectively.

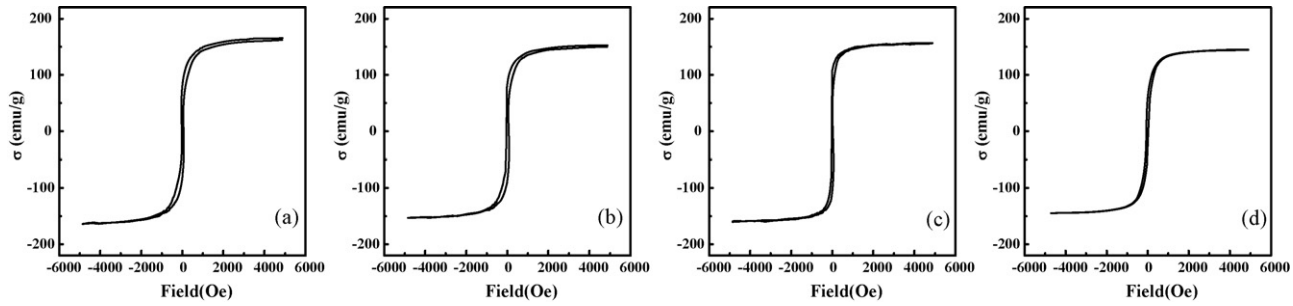

Fig. 3. Hysteresis loops for γ′-$(Fe_{1-x}Ni_x)_4N$ thin films with Ni concentration of (a) 0.05, (b) 0.25, (c) 0.36, and (d) 0.50, respectively.

is about 66 Oe at room temperature. The saturation magnetization of 166 emu/g is slightly smaller than the value of 186 emu/g for the pure γ′-Fe_4N film, reported by Coey [9], which can be ascribed to introducing Ni into the film since the magnetic moment of Ni ($M_{Ni} = 0.6\ \mu_B$) is smaller than that of Fe ($M_{Fe} = 2.2\ \mu_B$). It is worth mentioning that apart from the saturation magnetization, the coercivity is another important parameter for the magnetic functional materials. The coercivity for the film with different Ni concentrations is obviously smaller than that for pure γ′-Fe_4N film and decreases with increasing Ni concentration in the range of 0.05–0.36. However, the coercivity increases to 76 Oe when the Ni concentration increases up to 0.50. The coercivity is affected by the factors such as grain size, anisotropy, stress, surface roughness, etc. [29]. In general, nanocrystalline γ′-FeNiN films show in-plane magnetic uniaxial anisotropy [27,28]. Firstly, the change in the coercivity can be understood according to the relationship between the coercive force H_c and grain size D [30–31]: $H_c \propto 1/D$ when D is larger than the exchange length L_{ex}, $H_c \propto D^6$ when the grain size D is less than exchange length L_{ex}. Soft magnetic properties are related with the grain size. From this relationship, it can be deduced that the grain size D of γ′-$(Fe_{1-x}Ni_x)_4N$ thin films is larger than the exchange length L_{ex}, with increasing the grain size of γ′-$(Fe_{1-x}Ni_x)_4N$ thin films, H_c decreases, as Ni concentration increases from 0.05 to 0.36. On the other hand, as Ni concentration equals or is larger than 0.50, the increase in the coercivity can be explained from that Fe or Ni phase appears. From above, the soft magnetic properties can be optimized by controlling Ni concentration.

4. Conclusions

Nanocrystalline γ′-$(Fe_{1-x}Ni_x)_4N$ thin films with different Ni concentrations can be synthesized on single crystal Si(1 0 0) substrate by facing target magnetron sputtering. Via optimizing Ni concentration in γ′-$(Fe_{1-x}Ni_x)_4N$ thin films, their soft magnetic properties can be improved effectively. The improved soft magnetic properties can be attributed to the increase in grain size for γ′-$(Fe_{1-x}Ni_x)_4N$ thin films upon introducing Ni into Fe–N in a proper concentration.

Acknowledgements

The authors gratefully appreciate the financial support by the National Natural Science Foundation of China under Grant No. 50832001 and Ph.D. program under Grant No. 200801830025.

References

[1] W.T. Zheng, C.Q. Sun, Prog. Solid State Chem. 34 (2006) 1–20.
[2] T.K. Kim, M. Takahashi, Appl. Phys. Lett. 20 (1972) 492–494.
[3] J.F. Bobo, H. Chabi, M. Vergnat, et al., J. Appl. Phys. 77 (1995) 5309–5313.
[4] M.A. Abdellateef, C. Heiden, H. Lemke, F.M. El-Hossary, K. Baerner, J. Magn. Magn. Mater. 256 (2003) 214–220.
[5] Q. Zhan, R. Yu, L.L. He, D.X. Li, Thin Solid Film 411 (2002) 225–228.
[6] X. Luo, S. Liu, J. Magn. Magn. Mater. 191 (2007) L1–L4.
[7] T. Takahashi, N. Takahashi, et al., Solid State Sci. 6 (2004) 97–99.
[8] D.L. Peng, T. Hihara, K. Sumiyama, J. Alloys Compd. 207 (2004) 377–383.
[9] J.M.D. Coey, P.A.I. Smith, J. Magn. Magn. Mater. 200 (1999) 405–424.
[10] S. Grachev, D.M. Borsa, S. Vongtragool, D.O. Boerma, Surf. Sci. 482–485 (2001) 802–808.
[11] N.D. Telling, G.A. Jones, C.A. Faunce, P.J. Grundy, J. Vac. Sci. Technol. A19 (2001) 405–409.
[12] J.P. Zhou, D. Li, Y.S. Gu, et al., J. Magn. Magn. Mater. 238 (2002) L1–L5.
[13] S.Y. Grachev, D.M. Borsa, D.O. boerma, Surf. Sci. 515 (2002) 359–368.
[14] N. Takahashi, Y. Toda, T. Nakamura, Mater. Lett. 42 (2000) 380–382.
[15] H. Jacobs, D. Rechenbach, U. Zachwieja, J. Alloys Compd. 227 (1995) 10–17.
[16] L.L. Wang, X. Wang, N. Ma, W.T. Zheng, et al., Surf. Coat. Technol. 201 (2006) 786–791.
[17] J. Das, S.S. Kalarickal, K.S. Kim, et al., Phys. Rev. B 75 (2007) 094435.
[18] I. Fergen, K. Seemann, J. Magn. Magn. Mater. 242–245 (2002) 146–151.
[19] M. Kopcewicz, J. Jagielski, G. Gawlik, A. Grabias, J. Appl. Phys. 78 (1995) 1312–1321.
[20] R.N. Panda, N.S. Gajbhiye, J. Appl. Phys. 86 (1999) 3295–3302.
[21] N. Ishiwata, C. Wakabayashi, H. Urai, J. Appl. Phys. 69 (1991) 5616–5618.
[22] G. Qiu, E. Haftek, J.A. Barnard, J. Appl. Phys. 73 (1993) 6573–6575.
[23] H.Y. Wang, Z.W. Ma, E.Y. Jiang, Y.J. He, H.S. Huang, Appl. Phys. A 68 (1999) 559–562.
[24] H.Y. Wang, J. Liu, H.S. Huang, et al., J. Appl. Phys. 91 (2002) 1453–1457.
[25] X.G. Diao, A.Y. Takeuchi, F. Garcia, et al., J. Appl. Phys. 85 (1999) 4485–4487.
[26] P. Prieto, J. Camarero, N. Sacristan, et al., Phys. Stat. Sol. A 203 (2006) 1442–1447.
[27] P. Prieto, K.R. Pirota, J.M. Sanz, et al., Appl. Phys. Lett. 90 (2007), 0332505-1-3.
[28] X.F. Wang, P. Wu, X.J. Liu, Phys. Stat. Sol. A 205 (2008) 350–356.
[29] S.G. Wang, C.K. Ong, Z.W. Li, Phys. B 349 (2004) 129–135.
[30] L. Varga, H. Jiang, T.J. Kelmmer, W.D. Doyle, E.A. Payzant, J. Appl. Phys. 83 (1998) 5955–5966.
[31] W.H. Zhong, C.Q. Sun, S. Li, et al., Acta Mater. 53 (2005) 3207–3214.